

# Magnetic excitations from the edge-sharing $\text{CuO}_2$ chains in $\text{Ca}_2\text{Y}_2\text{Cu}_5\text{O}_{10}$

M. Matsuda

Advanced Science Research Center, Japan Atomic Energy Research Institute, Tokai, Ibaraki 319-1195, Japan

H. Yamaguchi, T. Ito, C. H. Lee, and K. Oka

Electrotechnical Laboratory, 1-1-4 Umezono, Tsukuba, Ibaraki 305-8568, Japan

Y. Mizuno, T. Tohyama, and S. Maekawa

Institute for Materials Research, Tohoku University, Sendai 980-8577, Japan

K. Kakurai

Neutron Scattering Laboratory, ISSP, University of Tokyo, Tokai, Ibaraki 319-1106, Japan

(Received 16 October 2000; published 19 April 2001)

Neutron inelastic scattering experiments were performed on the quasi-one-dimensional magnet  $\text{Ca}_2\text{Y}_2\text{Cu}_5\text{O}_{10}$ , which consists of the ferromagnetic edge-sharing  $\text{CuO}_2$  chains. The magnetic excitation peak width in energy becomes broader with increasing  $Q$  along the chain although sharp excitations are observed around the zone center and perpendicular to the chain. We revealed that the anomalous magnetic excitation spectra are caused mainly by the antiferromagnetic interchain interactions.

DOI: 10.1103/PhysRevB.63.180403

PACS number(s): 75.40.Gb, 75.30.Ds, 75.10.Jm

One-dimensional (1D) cuprates have been studied extensively because they are a good realization of spin  $\frac{1}{2}$  1D magnets, which show novel phenomena originating from quantum fluctuations. Recently, copper oxides with edge-sharing  $\text{CuO}_2$  chains, in which copper spins are coupled by the nearly  $90^\circ$  Cu-O-Cu interaction, were found to exhibit various interesting phenomena. The sign and the absolute value of the exchange interaction between copper spins depend sensitively on the bond angle and the distance between copper and oxygen ions.<sup>1</sup> The chains in  $\text{CuGeO}_3$  have an antiferromagnetic interaction and show a spin-Peierls transition at a low temperature.<sup>2</sup> On the other hand, in  $\text{Li}_2\text{CuO}_2$ , the  $\text{Cu}^{2+}$  spins order ferromagnetically in the chain below 9.3 K.<sup>3</sup> In  $\text{Sr}_{14}\text{Cu}_{24}\text{O}_{41}$ , the Cu ions in the chain show a unique dimerized state which is driven by a hole ordering.<sup>4-7</sup>

The  $\text{Ca}_{2+x}\text{M}_{2-x}\text{Cu}_5\text{O}_{10}$  ( $M=\text{Y}$ ,  $\text{Nd}$ , and  $\text{Gd}$ ) system consists of the edge-sharing  $\text{CuO}_2$  chains.<sup>8,9</sup> A schematic structure of the edge-sharing  $\text{CuO}_2$  chains is shown in Fig. 1. In the end material  $\text{Ca}_2\text{Y}_2\text{Cu}_5\text{O}_{10}$ , the  $\text{Cu}^{2+}$  ions align ferromagnetically along the chain ( $a$  axis) below  $\sim 29$  K.<sup>10,11</sup> The ferromagnetic chains are coupled ferromagnetically along the  $b$  axis and antiferromagnetically along the  $c$  axis. The ordered moment of copper is  $\sim 0.9\mu_B$  at low temperatures,<sup>10,11</sup> similar to the full magnetic moment of the free  $\text{Cu}^{2+}$  ion. An important feature of the edge-sharing  $\text{CuO}_2$  chain is a possible frustration between nearest-neighbor (NN) and next-nearest-neighbor (NNN) interactions.<sup>1</sup> Another characteristic feature of this compound is the existence of the antiferromagnetic interactions perpendicular to the chain.

In classical magnets, magnetic excitations are sharp throughout the whole Brillouin zone. However, frustration and interchain coupling affect the magnetic excitations in the coupled edge-sharing  $\text{CuO}_2$  chains, as reported by Mizuno, Tohyama, and Maekawa using the exact diagonalization technique.<sup>12</sup> They predicted that the magnetic excitations in

$\text{Li}_2\text{CuO}_2$  (Ref. 13) are well-defined around the zone center but the excitations become broader with increasing  $Q$  due to the combined effect of frustration by the NNN interaction and the quantum fluctuation by the interchain interaction. It has not been confirmed yet whether or not the calculation explains the experimental results. Therefore, it is important to study other compounds with the edge-sharing  $\text{CuO}_2$  chains in order to elucidate the validity of the calculation as well as the effect of frustration and the interchain interaction.

In this paper we studied the magnetic interactions in  $\text{Ca}_2\text{Y}_2\text{Cu}_5\text{O}_{10}$  using the neutron-scattering technique. It is found that the magnetic correlation in the long-range ordered state is realized to be commensurate because the NNN interaction is very small. However, the magnetic excitations are affected considerably. The excitation peak width in energy becomes broader with increasing  $Q$  along the chain although sharp excitations are observed around the zone center and perpendicular to the chain. This experimental result is reproduced qualitatively using the exact diagonalization technique. It is revealed that the anomalous broadening on the

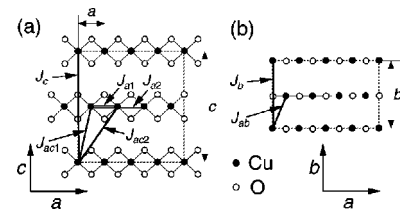


FIG. 1. Structure of the edge-sharing  $\text{CuO}_2$  chains in the  $ac$  plane (a) and in the  $ab$  plane (b). It is noted that oxygen ions are located at  $z \sim \pm 0.125$  in (b). Below  $T_N = 29.5$  K the  $\text{Cu}^{2+}$  spins align ferromagnetically along the chain ( $a$  axis) with the propagation vector  $\mathbf{k} = [001]$ .  $J_{a1}$ ,  $J_b$ ,  $J_c$ ,  $J_{ac1}$ , and  $J_{ab}$  are NN couplings along the  $a$  (chain),  $b$ ,  $c$ ,  $(1/2, 0, 1/2)$ , and  $(1/2, 1/2, 0)$  directions, respectively.  $J_{a2}$  is a NNN coupling along the  $a$  axis.  $J_{ac2}$  is a coupling along  $(3/2, 0, 1/2)$ .

magnetic excitations is caused mainly by the interchain interactions in  $\text{Ca}_2\text{Y}_2\text{Cu}_5\text{O}_{10}$ .

The single crystal of  $\text{Ca}_2\text{Y}_2\text{Cu}_5\text{O}_{10}$  was grown by the traveling solvent floating zone (TSFZ) method in air. The dimensions of the rod shaped crystal were  $\sim 6\Phi \times 25 \text{ mm}^3$ . The lattice constants were  $a = 2.810 \text{ \AA}$ ,  $b = 6.190 \text{ \AA}$ , and  $c = 10.613 \text{ \AA}$  at room temperature, which are consistent with those of the polycrystalline sample.<sup>8,9</sup>  $T_N$  is determined to be  $\sim 29.5 \text{ K}$  from the temperature dependence of the magnetic Bragg peak intensity, which is also consistent with that of the polycrystalline sample.<sup>10,11</sup> The detail of the crystal characterization is described elsewhere.<sup>14</sup>

The neutron-scattering experiments were carried out on the thermal neutron three-axis spectrometer ISSP-PONTA installed at JRR-3M at the Japan Atomic Energy Research Institute. The horizontal collimator sequence was  $40'-40'-S-40'-80'$  with the fixed final neutron energy  $E_f = 14.7 \text{ meV}$ . Contamination from higher-order beams was effectively eliminated using PG filters. The single crystal, which was oriented in the  $(HOL)$  or  $(HKO)$  scattering plane, was mounted in a closed cycle refrigerator.

Figure 2 shows the typical neutron inelastic spectra at  $(HOL)$  and  $(HKO)$  in  $\text{Ca}_2\text{Y}_2\text{Cu}_5\text{O}_{10}$  measured at  $7 \text{ K}$ . A sharp excitation peak is observed at  $(0,0,1)$  and  $(1,1,0)$ , which correspond to the magnetic zone center. The solid lines are the results of fits to a convolution of the resolution function with a Lorentzian  $\Gamma/[\Gamma^2 + (\omega - \omega_0)^2]$ , where  $\Gamma$  and  $\omega_0$  are inverse lifetime of magnetic excitations and excitation peak position, respectively.  $\Gamma$  is calculated to be less than  $0.1 \text{ meV}$  so that the peak width is resolution limited. The peak at  $(0,0,1)$  is slightly asymmetric and has a tail at higher energies due to the resolution effect. At  $(0.1,0,3)$  the excitation peak is still sharp and almost resolution limited. On the other hand, at  $(0.125,0,3)$  the excitation peak is broadened. The  $h$  dependence of  $\Gamma$  is shown in the inset of Fig. 3(a). With increasing  $h$ , the peak width becomes broader and no distinct excitation peak is observed above  $h = 0.2$ . On the other hand, the excitation peaks along the  $b$  and  $c$  axes are sharp and almost resolution limited as shown in Figs. 2(f) and 2(h). This indicates that the magnetic excitations are sharp around the zone center and perpendicular to the chain but become broader with increasing  $Q$  along the chain ( $a$  axis).

Figure 3 shows the observed excitation energies along  $h$ ,  $k$ , and  $l$ . As mentioned above, we could only observe low energy excitations along the chain ( $a$  axis) as shown in Fig. 3(a) since the excitations are broadened at higher  $Q$  and higher energies. Along the  $b$  and  $c$  axes, we determined the full dispersion relation as shown in Figs. 3(b) and 3(c). The dispersion along the  $b$  axis is almost flat, indicating that the interaction along the  $b$  axis is very small.

In order to analyze the observed dispersion relation we used a model Hamiltonian that includes uniaxial anisotropy:

$$H = \sum_{i,j} J_{i,j} \mathbf{S}_i \cdot \mathbf{S}_j + \sum_{i,j} J_{i,j}^z S_j^z \cdot S_j^z. \quad (1)$$

In the calculation of the dispersion relation, we introduced

$\text{Ca}_2\text{Y}_2\text{Cu}_5\text{O}_{10}$  14.7 meV, 40'-40'-40'-80'  $T=7 \text{ K}$

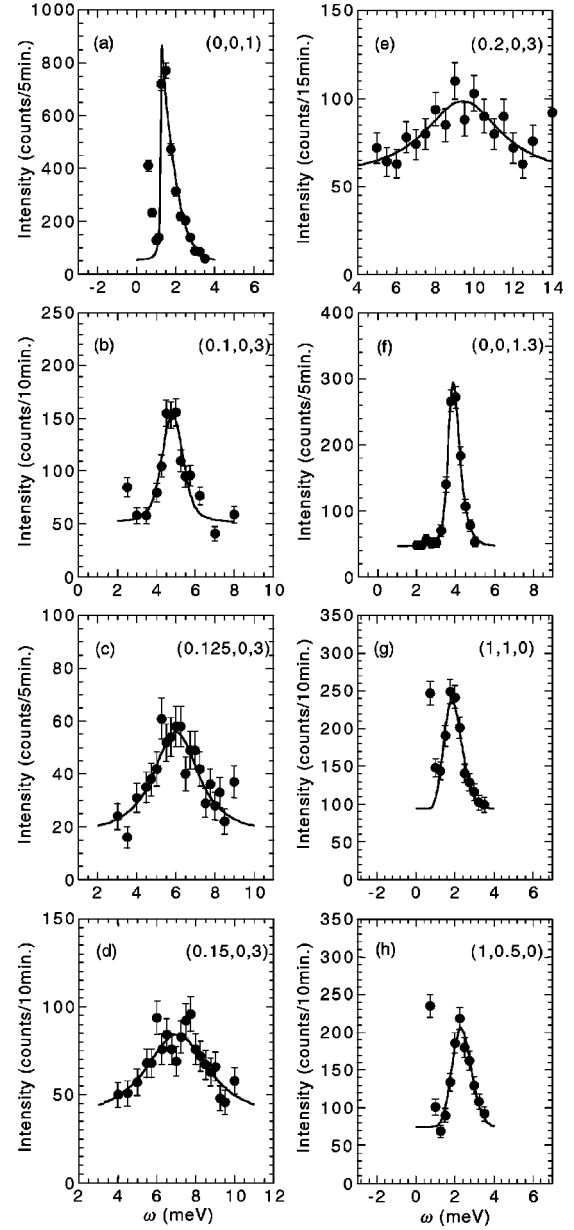


FIG. 2. Constant- $Q$  scans at  $(H,0,L)$  and  $(H,K,0)$  measured at  $T = 7 \text{ K}$  in  $\text{Ca}_2\text{Y}_2\text{Cu}_5\text{O}_{10}$ . The solid lines are the results of fits to a convolution of the resolution function with a Lorentzian. The scattering below  $1 \text{ meV}$  mostly originates from the incoherent scattering from the sample.

NN couplings  $J_{a1}$ ,  $J_b$ ,  $J_c$ ,  $J_{ac1}$ , and  $J_{ab}$  along the  $a$  (chain),  $b$ ,  $c$ ,  $(1/2,0,1/2)$ , and  $(1/2,1/2,0)$  directions, respectively. In addition to these interactions, a NNN coupling in the chain  $J_{a2}$ , a coupling along  $(3/2,0,1/2)$   $J_{ac2}$ , and the anisotropic interactions in the  $ac$  plane  $D_{ac}$  and in the  $ab$  plane  $D_{ab}$  are introduced. The interactions are shown in Fig. 1. From the consideration of the crystal structure and the orbital configuration, it is found that  $\frac{1}{2}J_{ac1} = J_{ac2}$ .<sup>12</sup> Applying the linear-spin-wave theory, the dispersion of the magnetic excitations is given by

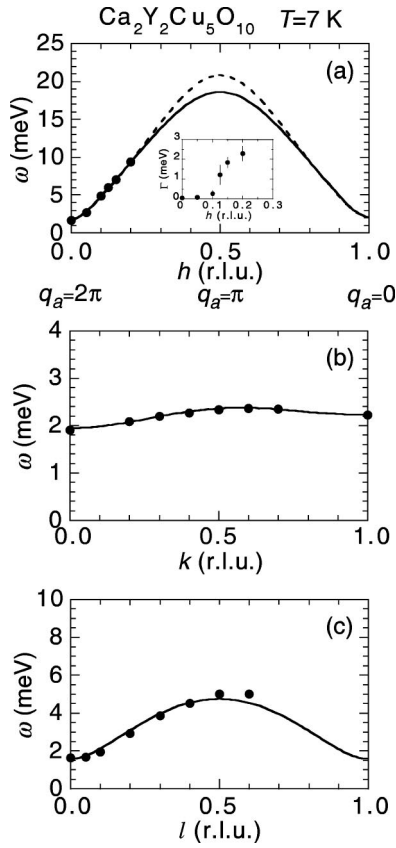


FIG. 3.  $\omega$ - $Q$  dispersion relation along the  $a$  (chain),  $b$ , and  $c$  axes for the edge-sharing  $\text{CuO}_2$  chain in  $\text{Ca}_2\text{Y}_2\text{Cu}_5\text{O}_{10}$ . The solid curves represent the theoretical ones with  $J_{a1} = -6.9$  meV,  $J_{a2} = 0$  meV,  $J_b = -0.061$  meV,  $J_c = 0$  meV,  $J_{ab} = -0.030$  meV,  $J_{ac1} = 1.494$  meV,  $J_{ac2} = 0.747$  meV. The anisotropic interactions are  $D_{ab} = -0.399$  meV in the  $(H, K, 0)$  zone (b) and  $D_{ac} = -0.262$  meV in the  $(H, 0, L)$  zone (a) and (c). The broken curve represents the theoretical one with  $J_{a1} = -8$  meV,  $J_{a2} = 0.4$  meV, and other interactions determined above. The inset in (a) shows the  $h$  dependence of the intrinsic peak width in energy ( $\Gamma$ ).

$$\omega(\mathbf{q}) = \left\{ \left[ J_{a1}(\cos q_a - 1) + J_{a2}(\cos 2q_a - 1) + J_b(\cos q_b - 1) \right. \right. \\ \left. \left. + J_c(\cos q_c - 1) + 2J_{ab} \left( \cos \frac{q_a}{2} \cos \frac{q_b}{2} - 1 \right) + 2J_{ac1} \right. \right. \\ \left. \left. + 2J_{ac2} - D \right]^2 - \left( 2J_{ac1} \cos \frac{q_a}{2} \cos \frac{q_c}{2} \right. \right. \\ \left. \left. + 2J_{ac2} \cos \frac{3q_a}{2} \cos \frac{q_c}{2} \right)^2 \right\}^{1/2}. \quad (2)$$

The dispersion along  $l$  in the  $(H, 0, L)$  zone can be calculated using only  $J_c$ ,  $J_{ac1}$ ,  $J_{ac2}$ , and  $D_{ac}$ . Since  $J_c$  is fitted to be almost 0, it is fixed at 0. The solid curve in Fig. 3(c) represents the result of a fit with  $J_{ac1} = 2J_{ac2} = 1.494(3)$  meV and  $D_{ac} = -0.262(3)$  meV. The calculated values reproduce the experimental result very well. The excitation gap at the zone center originates from the easy-axis uniaxial anisotropy along the  $b$  axis. At this momentum

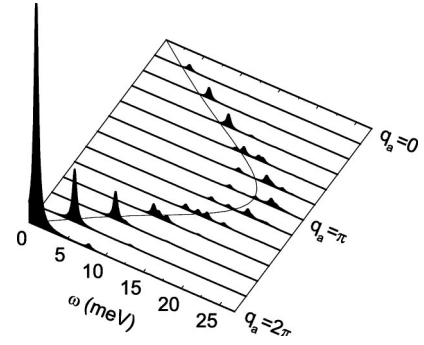


FIG. 4.  $S(\mathbf{q}, \omega)$  along the chain ( $a$  axis) with  $J_{a1} = -8$  meV,  $J_{a2} = 0.4$  meV, and  $J_{ac1} = 2J_{ac2} = 1.494$  meV. The system has  $12 \times 2$  sites, simulating the coupled edge-sharing chains in  $\text{Ca}_2\text{Y}_2\text{Cu}_5\text{O}_{10}$ . The  $\delta$  functions are convoluted with a Lorentzian broadening of 0.3 meV. The thin solid curve denotes a magnon dispersion obtained by the linear-spin-wave theory.

transfer  $(0, 0, 1)$  only spin fluctuations along the  $a$  axis are observed. We then calculated the dispersion along  $k$  in the  $(H, K, 0)$  zone. The solid curve in Fig. 3(b) represents the result of a fit with  $J_b = -0.061(6)$  meV,  $J_{ab} = -0.030(3)$  meV, and  $D_{ab} = -0.399(1)$  meV. In the fitting,  $J_{ac1}$  is fixed at 1.494 meV. At the zone center  $(1, 1, 0)$  scattering originates mainly from spin fluctuations along the  $c$  axis (99.2%).  $D_{ab}$  is slightly larger than  $D_{ac}$ , indicating that the twofold degeneracy of the spin wave branches is lifted because of the orthorhombic anisotropy. Finally, the dispersion along  $h$  in the  $(H, 0, L)$  zone is calculated. The solid line in Fig. 3(a) is the result of a fit with  $J_{a1} = -6.9(1)$  meV alone. Other interactions are fixed at the values determined above. Without using  $J_{a2}$ , the observed data are reproduced reasonably well. We then considered  $J_{a2}$  in addition to  $J_{a1}$ . The broken line in Fig. 3(a) is the result of a fit with  $J_{a1} = -8(1)$  meV,  $J_{a2} = 0.4(3)$  meV. Excitation energies around the zone boundary increase when antiferromagnetic NNN coupling is introduced. It is noted that both calculations reproduce the observed data at low energies equally well. Since we have no data around the zone boundary, it is difficult to distinguish which result is appropriate only from the calculations. However, it is revealed from the experiments that  $J_{a2}$  is small ( $J_{a2}/|J_{a1}| = 0.05(4)$ ) even if it exists.

An anomalous feature in the dispersion along the chain is that the excitation peak becomes broader with increasing  $Q$ . This behavior cannot be explained if only intrachain couplings are considered since  $J_{a2}$  is small.<sup>15</sup> The next step is to clarify whether or not the interchain coupling affects the magnetic excitations. For this purpose we have calculated  $S(\mathbf{q}, \omega)$  along the chain using the exact diagonalization method for a  $12 \times 2$  cluster. Detail of the procedure is described elsewhere.<sup>12</sup> The result of  $S(\mathbf{q}, \omega)$  is shown in Fig. 4. It is noted that  $D$ , which does not affect the spectral structure except the opening of a small gap,<sup>12</sup> is not included in the calculation. The excitation is well-defined around the zone center. However, at  $q_a \leq 1.5\pi$  ( $h \geq 0.25$ ) and at  $\omega > 10$  meV the excitations are broadened. This is consistent with the experimental result qualitatively, indicating that the interchain coupling affects the magnetic excitations in the

high energy region in  $\text{Ca}_2\text{Y}_2\text{Cu}_5\text{O}_{10}$ .

We compare the result in  $\text{Ca}_2\text{Y}_2\text{Cu}_5\text{O}_{10}$  with that in  $\text{Li}_2\text{CuO}_2$ .  $J_{a1}$  and  $J_{ac1}$  in  $\text{Ca}_2\text{Y}_2\text{Cu}_5\text{O}_{10}$  are similar to those calculated for  $\text{Li}_2\text{CuO}_2$  ( $J_1 = -8.6$  meV and  $J_c = 1.4$  meV, where  $J_1$  and  $J_c$  are NN coupling along the chain and major interchain coupling, respectively).<sup>12</sup> However, both the sign and the absolute value of  $J_1$  are different from those determined experimentally (0.24 meV).<sup>13</sup> Now it is revealed that antiferromagnetic interchain interaction affects the magnetic excitations considerably, it is natural to consider that in  $\text{Li}_2\text{CuO}_2$  magnetic excitations along the chain are also damped and no distinct peak is observed above  $\sim 2.5$  meV (Ref. 13) due to the interchain interaction. Since NNN coupling along the chain  $J_2$  is calculated to be  $\sim 40\%$  of  $|J_1|$  in  $\text{Li}_2\text{CuO}_2$ , which is much larger than in  $\text{Ca}_2\text{Y}_2\text{Cu}_5\text{O}_{10}$ , the magnetic excitations are damped at lower energies ( $\sim 2.5$  meV) in  $\text{Li}_2\text{CuO}_2$  due to the combined effect of frustration by the NNN interaction and the quantum fluctuation by the interchain interaction.

In this study it is revealed that the broadening of the magnetic excitations is a characteristic phenomenon in the spin  $\frac{1}{2}$  ferromagnetic chain coupled antiferromagnetically. This behavior has not been observed in weakly coupled antiferromagnetic chains. In order to elucidate whether or not this is characteristic only in the ferromagnetic chain, we calculated  $S(\mathbf{q}, \omega)$  also in antiferromagnetically coupled antiferromagnetic chains. It is found that broadening of the magnetic excitations is not distinct in this system and the broadening is predicted only around the zone boundary. It would be difficult to observe the broadening experimentally since additional scattering, which originates from the excitation con-

tinuum, is superposed. Details of the calculation will be published separately.<sup>16</sup>

We now consider interactions in  $\text{Ca}_2\text{Y}_2\text{Cu}_5\text{O}_{10}$ .  $J_{a2}$  is small and  $\sim 5\%$  of  $|J_{a1}|$ . This is consistent with the commensurate magnetic correlations in the long-range ordered state. This value is, however, much smaller than that calculated using the exact diagonalization method ( $J_{a2}/|J_{a1}| = 2.2$ ).<sup>1</sup> One reason for this discrepancy would be that the calculation was made on  $\text{Ca}_5\text{Cu}_6\text{O}_{12}$  which has the edge-sharing  $\text{CuO}_2$  chains similar to those in  $\text{Ca}_2\text{Y}_2\text{Cu}_5\text{O}_{10}$ . A detailed calculation of the exchange constants using the parameters appropriate for  $\text{Ca}_2\text{Y}_2\text{Cu}_5\text{O}_{10}$  will give a better result. Another possibility would be that the small  $J_{a2}$  originates from a slight lattice distortion in the chain, which could disturb the hopping between the NNN Cu sites so that  $J_{a2}$  is reduced. The sign and the absolute value of the major interchain coupling  $J_{ac}$  are similar to those of the interchain coupling in  $\text{Sr}_{14}\text{Cu}_{24}\text{O}_{41}$  [1.7 meV (Ref. 6) and 0.75 meV (Ref. 7)], which has an arrangement of the edge-sharing  $\text{CuO}_2$  chains similar to that in  $\text{Ca}_2\text{Y}_2\text{Cu}_5\text{O}_{10}$ . The anisotropic interactions  $D_{ab}$  and  $D_{ac}$ , which work to align the spins perpendicular to the chain plaquettes ( $b$  axis), are similar to that in  $\text{Li}_2\text{CuO}_2$  ( $-0.31$  meV).<sup>13</sup> Similar magnetic anisotropy is also observed in  $\text{La}_{14-x}\text{Ca}_x\text{Cu}_{24}\text{O}_{41}$ .<sup>17,18</sup>

In summary, we studied the magnetic interactions in  $\text{Ca}_2\text{Y}_2\text{Cu}_5\text{O}_{10}$  using the neutron-scattering technique. It is revealed that  $J_{a2}$  is small. The most characteristic feature is that the magnetic excitations are broadened considerably at high  $Q$ 's and high energies mainly due to the interchain interaction. This is characteristic in the spin  $\frac{1}{2}$  ferromagnetic chain coupled antiferromagnetically.

<sup>1</sup>Y. Mizuno, T. Tohyama, S. Maekawa, T. Osafune, N. Motoyama, H. Eisaki, and S. Uchida, Phys. Rev. B **57**, 5326 (1998).

<sup>2</sup>M. Hase, I. Terasaki, and K. Uchinokura, Phys. Rev. Lett. **70**, 3651 (1993).

<sup>3</sup>A. Sapiña, J. Rodríguez-Carvajal, M. J. Sanchis, R. Ibanez, A. Beltran, and D. Beltran, Solid State Commun. **74**, 779 (1990).

<sup>4</sup>M. Takigawa, N. Motoyama, H. Eisaki, and S. Uchida, Phys. Rev. B **57**, 1124 (1998).

<sup>5</sup>R. S. Eccleston, M. Uehara, J. Akimitsu, H. Eisaki, N. Motoyama, and S. Uchida, Phys. Rev. Lett. **81**, 1702 (1998).

<sup>6</sup>L. P. Regnault, J. P. Boucher, H. Moudden, J. E. Lorenzo, A. Hiess, U. Ammerahl, G. Dhalenne, and A. Revcolevschi, Phys. Rev. B **59**, 1055 (1999).

<sup>7</sup>M. Matsuda, T. Yoshida, K. Kakurai, and G. Shirane, Phys. Rev. B **59**, 1060 (1999).

<sup>8</sup>P. K. Davis, E. Caignol, and T. King, J. Am. Ceram. Soc. **74**, 569 (1991).

<sup>9</sup>P. K. Davis, J. Solid State Chem. **9**, 365 (1991).

<sup>10</sup>M. Matsuda, K. Ohya, and M. Ohashi, J. Phys. Soc. Jpn. **68**, 269 (1999).

<sup>11</sup>H. F. Fong, B. Keimer, J. W. Lynn, A. Hayashi, and R. J. Cava, Phys. Rev. B **59**, 6873 (1999).

<sup>12</sup>Y. Mizuno, T. Tohyama, and S. Maekawa, Phys. Rev. B **60**, 6230 (1999).

<sup>13</sup>M. Boehm, S. Coad, B. Roessli, A. Zheludev, M. Zolliker, P. Böni, D. McK. Paul, H. Eisaki, N. Motoyama, and S. Uchida, Europhys. Lett. **43**, 77 (1998).

<sup>14</sup>H. Yamaguchi, K. Oka, and T. Ito, Physica C **320**, 167 (1999).

<sup>15</sup>We calculated  $S(\mathbf{q}, \omega)$  without including interchain couplings. It is found that the broadening of the excitations is not expected only with  $J_{a1}$  and the small  $J_{a2}$ .

<sup>16</sup>T. Tohyama and S. Maekawa (unpublished).

<sup>17</sup>M. Matsuda, K. Katsumata, T. Yokoo, S. M. Shapiro, and G. Shirane, Phys. Rev. B **54**, R15 626 (1996).

<sup>18</sup>M. Matsuda, K. M. Kojima, Y. J. Uemura, J. L. Zarestky, K. Nakajima, K. Kakurai, T. Yokoo, S. M. Shapiro, and G. Shirane, Phys. Rev. B **57**, 11 467 (1998).